FREQUENCY-DOMAIN STRESS PREDICTION ALGORITHM FOR THE LIFE2 FATIGUE ANALYSIS CODE*

by

H. J. Sutherland
Wind Energy Research Division
Sandia National Laboratories
Albuquerque, NM 87185

SAND--91-0821C

DE92 000247

ABSTRACT

The LIFE2 computer code is a fatigue/fracture analysis code that is specialized to the analysis of wind turbine components. The numerical formulation of the code uses a series of cycle count matrices to describe the cyclic stress states imposed upon the turbine. However, many structural analysis techniques yield frequency-domain stress spectra and a large body of experimental loads (stress) data is reported in the frequency domain. To permit the analysis of this class of data, a Fourier analysis module has been added to the code. The module transforms the frequency spectrum to an equivalent time series suitable for rainflow counting by other modules in the code. This paper describes the algorithms incorporated into the code and uses experimental data to illustrate their use.

INTRODUCTION

The analysis of the fatigue lifetime of a component for a Wind Energy Conversion System (WECS) requires that the stress state imposed upon that component be formulated in terms of stress cycles. However, many structural analysis techniques yield frequency-domain stress spectra and a large body of experimental loads (stress) data is reported in the frequency domain. To permit the analysis of this class of data, a Fourier analysis module has been added to the LIFE2 fatigue/fracture analysis code [1]. The computational framework for this module follows the work of Akins [2]. Simply stated, the module converts frequency-domain stress data into time-series data (stress-time history) suitable for rainflow counting. The addition of this module to the LIFE2 code permits the code to predict the fatigue life of WECS components based upon the analysis of experimental and/or analytical frequency-domain stress spectra.

This manuscript describes the algorithms used in this computational module to convert the frequency-domain data into time-series data. The algorithms are illustrated by the examination of frequency-domain stress spectra from the Sandia 34-m Test Bed vertical axis wind turbine.

---

*This work is supported by the U.S. Department of Energy at Sandia National Laboratories under contract DE-AC04-76DP00789.

THE FFT ALGORITHM

To convert a frequency spectrum into a time series requires the use of an inverse Fourier transform. Several Fast Fourier Transforms (FFT's) and their inverses have been written, e.g., see Reference 3, that specialize the Fourier transform and its inverse into a "fast" digital analysis. One such transform [4], with its accompanying pre- and post-processors, has been incorporated into a LIFE2 computation module.

The LIFE2 module assumes that the input frequency spectrum is a uniform series of N components with a frequency interval of $\Delta\omega$. The spectrum is input as a series of positive amplitudes A_i and phase angles ϕ_i , i = 1, N. If a ϕ_i is not included in the input, a random number generator [5] is used to generate a random phase angle between 0 and 2π radians (see the discussion entitled "Random Phase Angle," below, for an explanation and analysis of the use of random phase angles to synthesize "realistic" time series data for wind turbines).

The FFT pre-processor reads the spectrum, generates random phases when required, and converts each phase into its sine and cosine components, $(A_i)_S$ and $(A_i)_C$, respectively, using the relations:

$$(A_i)_S = (A_i) \sin (\phi_i) \ , \qquad (1)$$

and,

$$(A_i)_C = (A_i) \cos (\phi_i) \ . \qquad (2)$$

The i^{th} component of the spectrum corresponds to a frequency of:

$$\omega_i = (i - 1) \Delta\omega \ , \text{ where } i = 1, \ldots, N. \qquad (3)$$

To speed processing, the mean stress (the zero frequency component A_1) is set equal to zero and the number of components in the spectrum, N, is set to a power of 2; i.e.,

$$A_1 = (A_1)_S = (A_1)_C = 0 \ , \qquad (4)$$

and

$$N = 2^m \ , \text{ where } m \text{ is a positive integer.} \qquad (5)$$

If the input value of N is not a power of 2, the additional components in the amplitude spectrum are set equal to zero.

The inverse FFT algorithm converts this frequency spectrum into a time series [3]. The output time series is a uniform series, with the time increment, $\Delta\tau$, given by:

$$\Delta\tau = \frac{1}{2\,N\,\Delta\omega} \,. \qquad (6)$$

The FFT post-processor adds the mean stress to the time series and writes the results to file in a format suitable for analysis by the rainflow counter in the LIFE2 code [6]. The output time series has a total time length T equal to

$$T = 2\,N\,\Delta\tau = \frac{1}{\Delta\omega} \,. \qquad (7)$$

THE 34-m FREQUENCY SPECTRUM

To illustrate the use of this set of algorithms and to validate their implementations in the LIFE2 code, consider the typical stress-time history shown in Figure 1. These data were measure on the Sandia/DOE 34-m Test Bed Vertical Axis Wind Turbine (VAWT) located near Bushland, TX [7]. They are flatwise blade stresses at the upper blade-to-tower joint for a wind speed interval of 12 to 15 m/s. These data were taken with the turbine rotating with a constant speed of 0.47 Hz (28 rpm). A detailed rainflow analysis of these and similar data are presented in Reference 8.

Figure 1 shows the first 100 seconds of a 700-second stress-time history. The 700 second record has a root-mean-square (RMS) of 6.2 MPa and an average of - 1.0 MPa [8]. These statistics compare well to the "bins" data for this same wind speed interval with a 6.6 MPa RMS and a -1.1 MPa mean [7].

The time history shown in Figure 1 was analyzed using both the FFT used here [4] and the FFT contained in the Sandia Data Acquisition and Analysis System [7]. The results of the two analyses are identical, within numerical accuracy.

The frequency-domain amplitude spectrum for the first 51.2 seconds of the record is shown in Figure 2. The time series data are taken with a $\Delta\tau$ of 0.05 seconds. Thus, the first 1024 (2^{10}) time-series data points are analyzed. Using Equation 6, the amplitude spectrum is a uniform series with a $\Delta\omega$ of 0.0195 Hz. The 512 amplitudes span a frequency range from 0 and 10 Hz (only the range 0 to 6 Hz is shown in Figure 2).

An average spectrum for the entire time-series data set was obtained by computing the amplitude spectrum for 13 sequential data blocks, each 51.2 seconds long, and averaging the amplitude at each ω_i. The resulting "average" amplitude spectrum is shown in Figure 3. The variation about the mean at each ω_i was ±88 percent, with no excursions greater than 1 MPa.

The frequency spectrum shown in Figure 3 was filtered to remove all components with amplitudes below 0.2 MPa. The resulting spectrum is shown in Figure 4. This spectrum will be used below to illustrate the influence of the relatively small amplitude components on the FFT algorithm and its rainflow counted stress cycles.

VALIDATION

In addition to preliminary validations of the algorithms using single and multiple sine and cosine waves, the time series shown in Figure 1 was used for validation. The first 51.2 seconds of this record were transformed using an FFT [4]. The resulting sine and cosine components were then converted to amplitude and phase components using Equations 1 and 2 (the amplitude spectrum is shown in Figure 2). The amplitudes and phases were then synthesized into a time series using the LIFE2 code. Comparing the initial time series to the synthesized time series yields a point-by-point average difference between the two of 0.0000049 MPa, a variance of 0.000058 MPa^2 and a standard deviation of 0.0076 MPa. Thus, the initial and synthesized time series are identical, within numerical roundoff.

SYNTHESIZED RAINFLOW CYCLE COUNTS

As discussed above, the algorithms that have been added to the LIFE2 code permit a stress-time history to be synthesize from a frequency spectrum of the stress imposed upon a turbine component, and then to be rainflow counted to determine the stress cycles imposed on that component. To illustrate this capability, the spectra for the 34-m Test Bed, discussed above, will be used.

Time-Series Data: The time-series data cited above and shown in Figure 1 have been previously rainflow counted [8]. The resulting stress cycle counts for the entire 700-second record are shown in Figure 5. To permit direct comparisons of the data, the distribution of cycle counts in this figure has been normalized to 100 seconds, and the counts in the low stress region are not shown. Also shown in Figure 5 is the narrow band Gaussian model that has been proposed by Veers [9]. These data and the prediction for the model will be cited throughout the remainder of this report to illustrate the capabilities of the frequency-domain analysis.

As noted previously [8], the essential difference between the time-series and the narrow band Gaussian model is that the former is based on 700 seconds of data while the latter is based on a model that uses "bins" data from many thousands of seconds of turbine operation. The difference is noted in the RMS of the data and by the presence of cycle counts in the "high-stress" tail of the distribution. The time series has an RMS of 6.2 MPa and the narrow band Gaussian model has an RMS of 6.6 MPa. The high-stress tail is sparsely populated by the time-series counts. As discussed in References 8 and 10, the distribution of the cycle counts in the high-stress tail is very significant in the determination of the service lifetime for turbine components.

Resynthesis: As discussed above, if the amplitude and phase for each of the 13 blocks of data are input into the LIFE2 code, the algorithms used here will duplicate the time series data within numerical accuracy. And, the cycle counts shown in Figure 5 are duplicated.

Random Phase: Typically, frequency spectra from wind turbines contain two classes of signals. The first is the "steady" signal that is obtained by averaging the time series data as a function of rotor position (the azimuthal average). The second signal in the spectrum is a random variation about the azimuthal average. The random components in the distribution imply that the synthesis of a time series from a frequency spectrum for wind turbines is not a unique process.

Akins [2] handled the synthesis of both signals using the average amplitude spectrum with a random phase angle for each amplitude. He suggests that a synthesized time series would be closer to an actual measured time series if the phase angles for the azimuthal-averaged components of the spectra are included in the synthesis; i.e., because the phase angles for azimuthal-averaged components are essentially constant, they should be included in the synthesis process. And he further suggests that the random components are best described using the average amplitude spectrum with random phases.

The concept of fixed and random phase angles has been incorporated into the LIFE2 algorithms using variable input parameters. When the amplitude spectrum is entered into the code, an algorithm examines the input to determine if an associated phase angle is included for each amplitude. If a phase angle is included, the code will use that phase angle. If a phase angle is not included, the code generates a random phase for that component of the amplitude spectrum.

The following sections illustrate the use of these algorithms on the spectral data for the 34-m Test Bed that is cited above.

Random Phase: The average amplitude spectrum, Figure 3, was input into the algorithm with no phase angles included. The LIFE2 code generated random phase angles for all of the amplitude components. The resulting time series was then counted using the rainflow counter. The process was repeated many times, with different, random phase angles. Each time series, 51.2 seconds in length, was "attached" to the end of the previous time series. The cycle count matrix stabilized at 5120 seconds; i.e., the number of cycle counts in each stress bin at 5120 second (100 repeats of the time series synthesis) was within 0.5 cycle of the cycle counts at 10,240 second (200 repeats). The cycle counts for 1024, 2560 and 5120 seconds are shown in Figure 6. The cycle counts for 5120 seconds are compared to the time series data and the narrow band Gaussian model in Figure 7.

High-Amplitude Phase: In a similar calculation, the phase angles for the high-amplitude components were included in the input. Specifically, the phase angle for the three peaks near 0.5, 1.0 and 1.4 Hz were included in the input data. These peaks correspond to the first, second and third multiples of the rotational speed of the turbine (0.47 Hz). All other phase angles remained random. The synthesis process again stabilized at 5120 seconds (100 repeats). Figure 8 compares the cycle counts from this synthesis to the time series data and the narrow band Gaussian model.

Discussion: As seen in the comparison of Figures 7 and 8, the inclusion of the phase angles on the high-amplitude components of the spectrum changed the cycle counts only slightly from those obtained with all random phases. In both cases, the cycle counts closely followed the cycle counts from the original time series of 700 seconds in the main body of the distribution. However, in the high-stress tail of the distribution, all random phases yield cycle counts out to the 58-60 MPa bin, while the high-amplitude phase synthesis yields counts out to the 48-50 MPa bin.

Amplitude Variations: As discussed above, the single-series amplitude spectra (Figure 2) varied significantly about the average spectrum (Figure 3). Two classes of variations are noted: the first is the variation of the spectral amplitudes about their average and the second is the variation of the RMS of the spectral amplitudes with wind speed.

Variation in Spectral Amplitudes: The amplitude spectrum for the 13 sequential data blocks varied about their mean by ± 88 percent with no excursions greater than 1 MPa. Using the random number generator, the amplitude of the input spectrum was varied in this manner. The resulting cycle count matrix stabilized at 5120 seconds and was essentially identical to the counts shown in Figure 7 when no phase angles were included and to that shown in Figure 8 when the high-amplitude phase angles were included.

Variation with Wind Speed Interval: The spectra cited above are based on a wind speed interval of 12 to 15 m/s; namely, for this data set, the wind speed varied between 12 and 15 m/s, with an average wind speed of 13.5 m/s [8]. Thus, the RMS of 6.2 MPa for the input time series and the average frequency spectrum (Figure 3) is based on a relatively large wind speed bin. Bins data from the 34-m Test Bed [7] indicate the RMS varies 36 percent across this wind speed range.

To investigate the influence of this variable, the RMS of the input frequency spectrum was systematically varied ± 18 percent about the mean. The mean root-mean-squared $(RMS)_m$ was changed by multiplying all amplitudes in the mean frequency spectrum, $(A_i)_m$, by a factor R_a; namely:

$$A_i = R_a\,(A_i)_m \text{ , where } i = 1, \ldots, N. \qquad (8)$$

Thus, the root-mean-square $(RMS)_a$ for the adjusted amplitude spectrum becomes:

$$(RMS)_a = \sqrt{\sum_{i=1}^{N} \frac{\left[\, R_a\,(A_i)_m \,\right]^2}{2}} \,, \qquad (9)$$

$$(RMS)_a = R_a \sqrt{\sum_{i=1}^{N} \frac{\left[\, (A_i)_m \,\right]^2}{2}} \,, \qquad (10)$$

$$(RMS)_a = R_a\,(RMS)_m \quad . \qquad (11)$$

For the synthesis presented here, R_a was varied between 0.82 and 1.18 in 100 equal increments. This variation used the spectrum shown in Figure 3 with the phase angle for the high-amplitude components included in the input. The resulting cycle counts for this synthesis are compared to the time series data and the narrow band Gaussian

model in Figure 9. The logarithmic plot of these data are presented in Figure 10. As noted in these figures, many hours of synthesized time series data were required to achieve a stable cycle count matrix.

Low Amplitude Components: Even the average spectrum, shown in Figure 3, contains a relatively high percentage of low amplitude components. To investigate the importance of these components, the spectrum was filtered to remove all components with amplitudes less than 0.2 MPa, see Figure 4. Using this spectrum with the high-amplitude phase included and incorporating the ± 18 percent variation in the RMS for the relatively large wind speed interval, the synthesized time series produced the cycle count matrix summarized in Figure 11. For comparison, the time series data and the narrow band Gaussian model are also shown in the figure. As illustrated in this figure, the elimination of the relatively small signals from the average spectrum significantly reduces the cycle counts in the entire cycle count matrix.

High-Stress Tail

As discussed in References 8 and 10, the population of cycle counts in the high-stress tail on the cycle count distribution is very important in the determination of the service lifetime of a turbine component. The original time series of 700 seconds contained cycle counts out to the 58-60 MPa alternating stress cycle bin, but with a sparse population, see Figure 10. The synthesized time series, cited in Figures 9 and 10 also contains counts out to the 58-60 MPa bin, and, importantly, the distribution in the high-stress tail is not sparsely populated. To achieve a stable, relatively smooth, and monotonically decreasing distribution of the cycle counts in the high-stress tail, over 100,000 seconds of time-series data had to be synthesized. Thus, the ability of the algorithm to generate relatively long time series permits this high-stress tail to be defined.

When the counts in the high-stress tail of the synthesized time series data are compared to the counts predicted by the narrow-band Gaussian model, see Figure 10, the time series underpredicts the counts in the tail. The reduced population in the high-stress tail is a direct results of the variation in the RMS value between the relatively long-time bins data and the relatively short-time frequency spectrum. As noted above, the bins data had an RMS value of 6.6 MPa and the frequency spectrum had an RMS value of 6.2 MPa. The bins RMS is based on many thousands of seconds of turbine operation while the frequency spectrum is based on 700 seconds of data.

In summary, the ability of the synthesized time-series technique to fill the tail of the cycle count distribution should not be confused with the actual distribution of stress cycles imposed upon the turbine. As exemplified by the RMS values and illustrated in Figure 10, the 700-second record does not describe the high-stress tail of the distribution of cycle counts. Thus, the frequency spectrum that is based on it does not contain sufficient information to define the high-stress tail of the cycle-count distribution, either.

Discussion

Based on the comparisons presented in Figures 6 through 11, the synthesis of time series data from average frequency-spectra data is an effective technique for the determination of stress cycles imposed on a wind turbine component. The data analyzed here indicate that the fixed-phase angle components significantly affect the

tail of cycle count distribution but not the main body of the distribution. Random amplitude variations about their mean have little or no effect on the cycle count distribution. And, the elimination of the small amplitude components of the spectrum reduces the cycle counts throughout the distribution. For relatively large wind speed intervals, the variation of the RMS in the amplitude spectrum with wind speed should be included in the synthesis process.

The ability of the algorithm to generate long time series permits the high-stress tail of the cycle count distribution to be defined.

SUMMARY

A set of algorithms permitting the analysis of frequency-domain stress data has been incorporated into the LIFE2 fatigue/fracture analysis code. The algorithms are based on the transform of frequency-domain, amplitude and phase spectra into time series data using a FFT. The algorithm permits the inclusion of fixed and/or random phase angles for the input spectrum, as deemed appropriate by the operator. Data from the 34-m Test Bed was used to illustrate the use of these algorithms and to investigate the effects of the various input parameters on the resulting cycle count matrix.

ACKNOWLEDGEMENTS

The author wishes to thank R. E. Akins for his help with this analysis. He supplied his original frequency-domain analysis [2], and discussed the nuances of his technique with me. The author also wishes to thank P. S. Veers for many helpful discussions concerning this analysis technique. R. L. Linker provided programming support for this project.

BIBLIOGRAPHY

1. Sutherland, H. J., and L. L. Schluter, "The LIFE2 Computer Code, Numerical Formulation and Input Parameters," *Proceedings of WindPower '89*, SERI/TP-257-3628, September 1989, pp. 37-42.

2. Akins, R. E., *Rainflow Counting Based on Predicted Stress Spectra*, Presented at the Eighth ASME Wind Energy Symposium, Houston, 1989.

3. Ramirez, R. W., *The FFT, Fundamentals and Concepts*,Prentice Hall, Englewood, 1985.

4. Jones, R. E., *FFT Subroutines*, Sandia Mathematical Program Library, Ver. 8.1, Albuquerque, 1980, (based on the algorithms developed by N. M. Brenner, MIT Lincoln Lab, and Cooley, Lewis and Welsh, IBM).

5. Jones, R. E., *Random Number Generator*, Sandia Mathematical Program Library, Albuquerque, 1980,

6. Schluter, L. L., and H. J. Sutherland, "Rainflow Counting Algorithm for the LIFE2 Fatigue Analysis Code," *Proceedings of the Ninth ASME Wind Energy Symposium*, D. E. Berg (ed), SED-Vol. 9, ASME, January 1990, pp. 121-123.

7. Ashwill, T. D., et. al., "The Sandia 34-Meter VAWT Test Bed," *Proceedings of Wind Power '87*, American Wind Energy Association, SERI/CP-217-3315, October 1987, pp. 298-308.

8. Sutherland, H. J., and L. L. Schluter, "Fatigue Analysis of WECS Components Using a Rainflow Counting Algorithm," *Proceedings of Windpower '90*, September 1990.

9. Veers, P. S., "Simplified Fatigue Damage and Crack Growth Calculations for Wind Turbines," *Proceedings of the Eight ASME Wind Energy Symposium*, D. E. Berg and P. C. Klimas (eds), SED-Vol. 7, ASME, January 1987, pp. 133-140.

10. Malcolm, D. J., "Predictions of Peak Fatigue Stresses in a Darrieus Rotor Wind Turbine Under Turbulent Winds," *Proceedings of the Ninth ASME Wind Energy Symposium*, D. E. Berg (ed), SED-Vol. 9, ASME, January 1990, pp. 125-135.

Figure 1. Typical Time History Data Record for the Sandia 34-m Test Bed Wind Turbine.

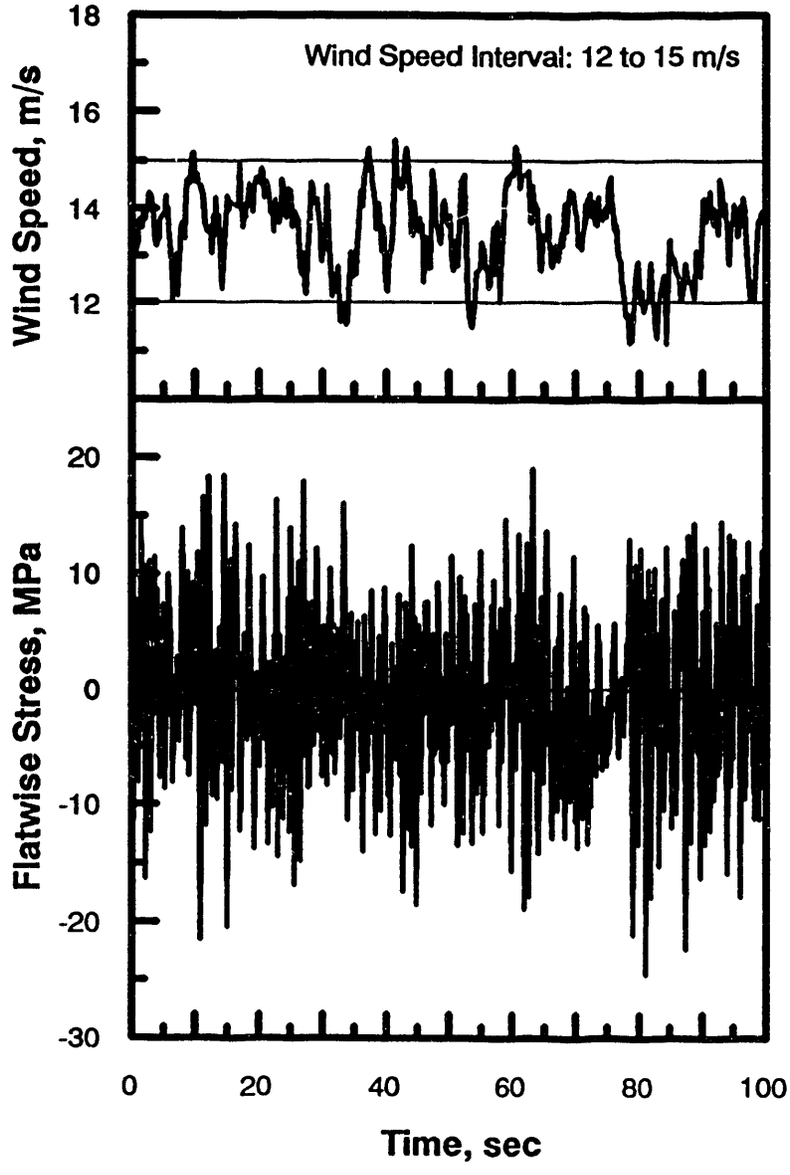

Figure 2. Single-Time-Series Amplitude Spectrum for the Sandia 34-m Test Bed.

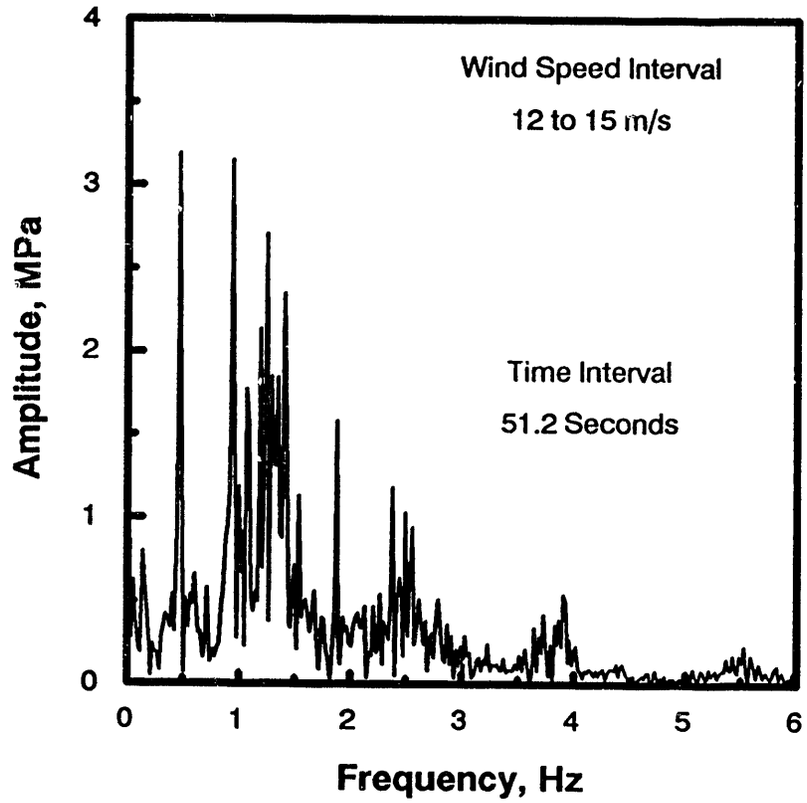

Figure 3. Average Amplitude Spectrum for the Sandia 34-m Test Bed.

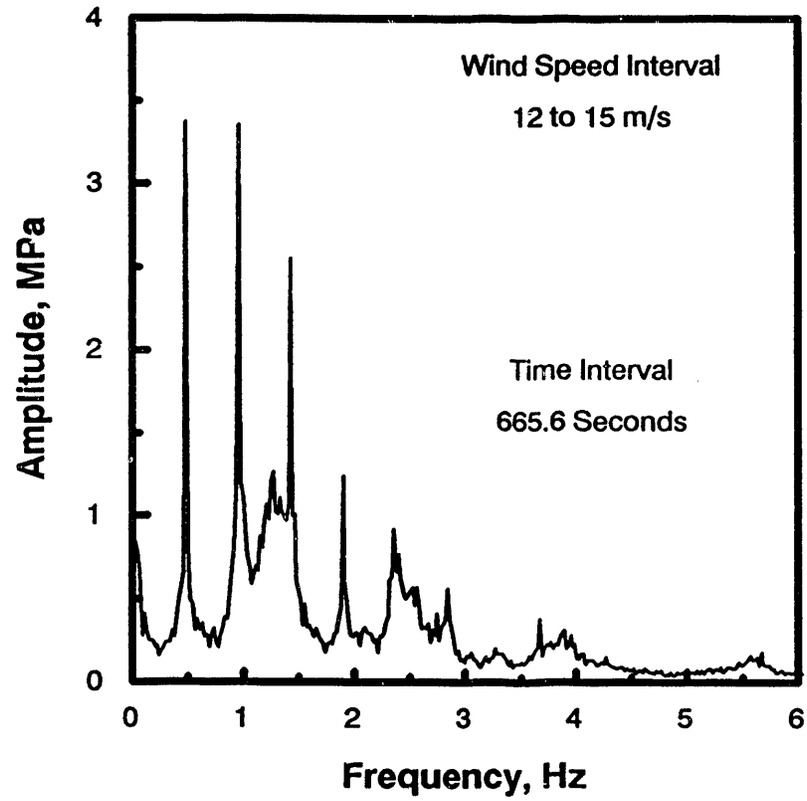

Figure 4. Average Amplitude Spectrum for the Sandia 34-m Test Bed with Small-Amplitude Phases Removed.

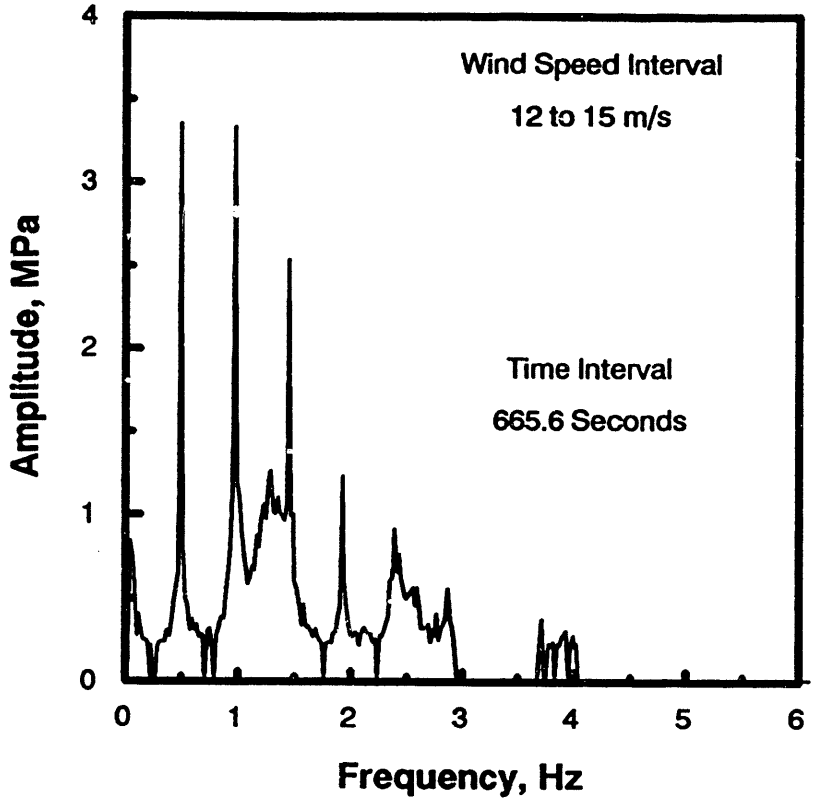

Figure 5. Cycle Counts for the 700-Second Stress-Time History from the Upper Blade-to-Tower Joint on the Sandia 34-m Test Bed.

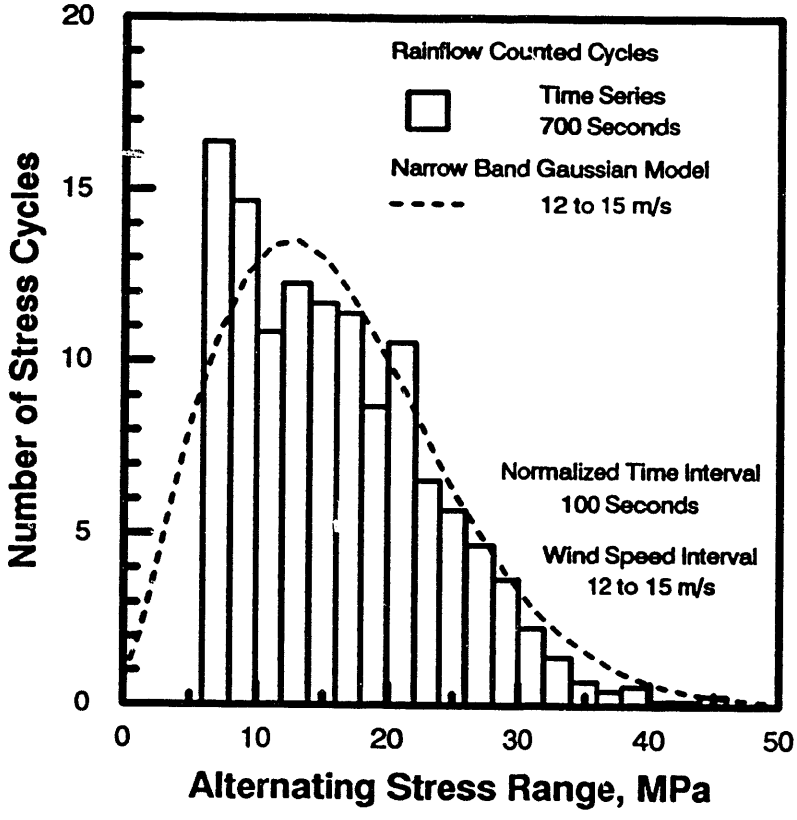

Figure 6. Cycle Counts for Time Series Synthesized from the Average Amplitude Spectrum with no Phase Angle.

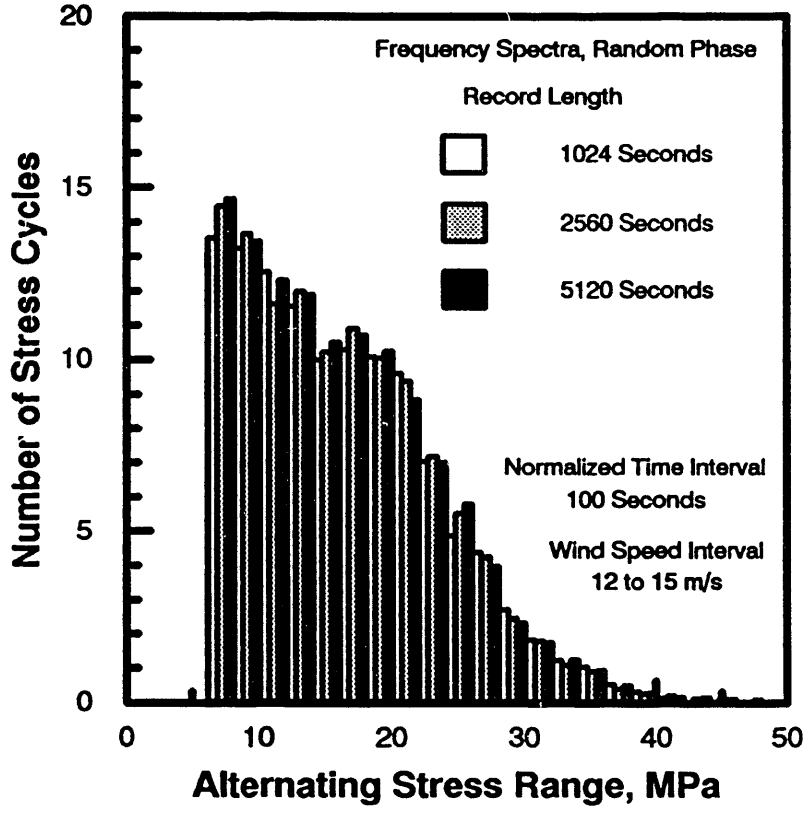

Figure 7. Cycle Counts for Time Series Synthesized from the Average Amplitude Spectrum with no Phase Angle.

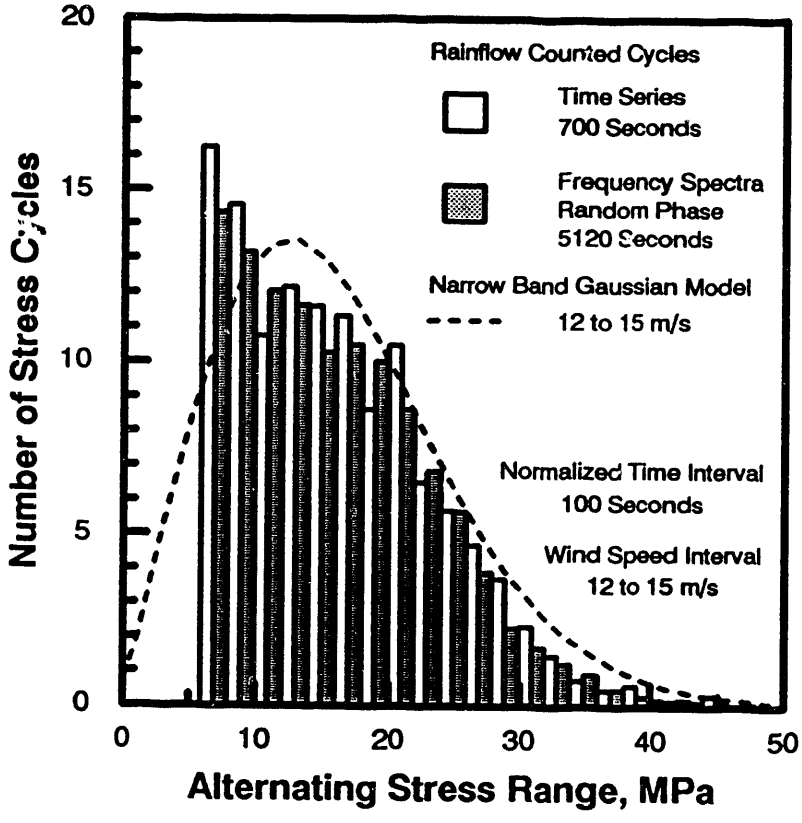

Figure 8. Cycle Counts for Time Series Synthesized from the Average Amplitude Spectrum with Phase Angles on the High-Amplitude Components.

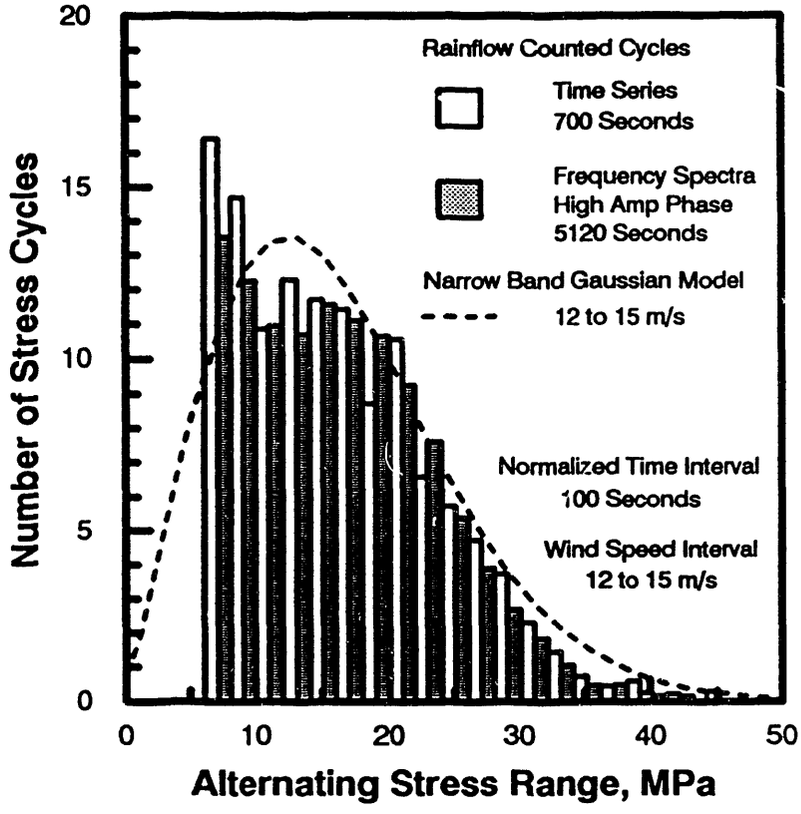

Figure 9. Cycle Counts for Time Series Synthesized with the RMS of the Input Frequency Spectrum Varying ±18 Percent.

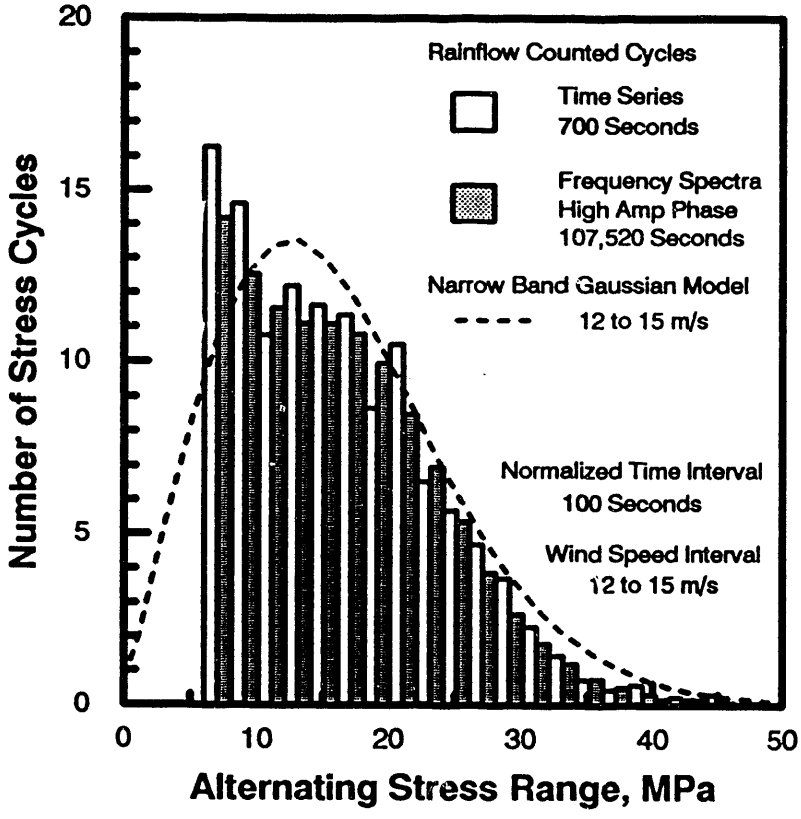

Figure 10. Cycle Counts for Time Series Synthesized with the RMS of the Input Frequency Spectrum Varying ±18 Percent; Logarithmic Scale.

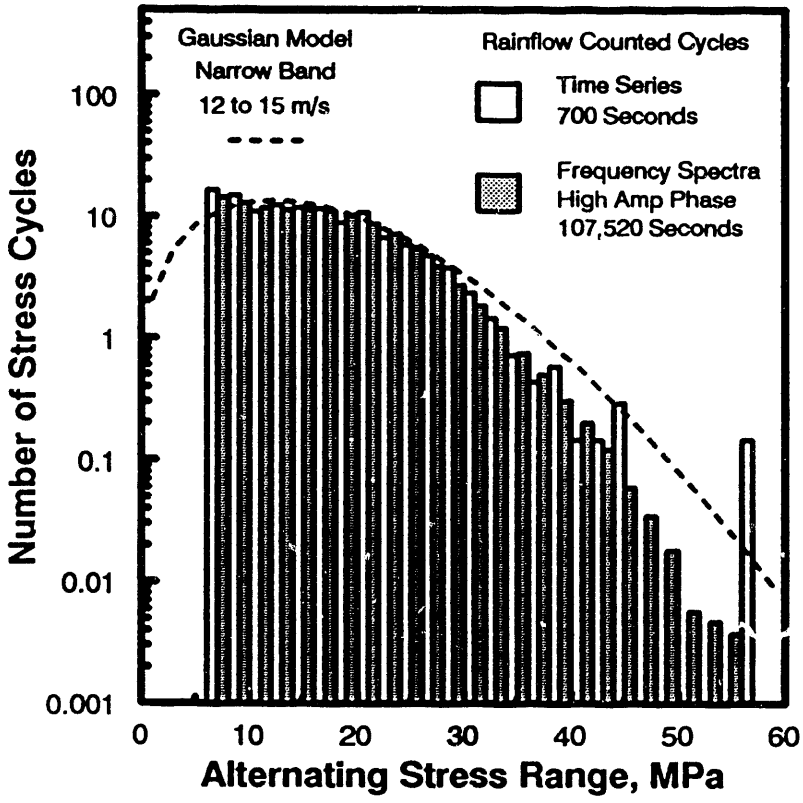

Figure 11. Cycle Counts for Time Series Synthesized with the Relative Small Amplitude Components Eliminated.

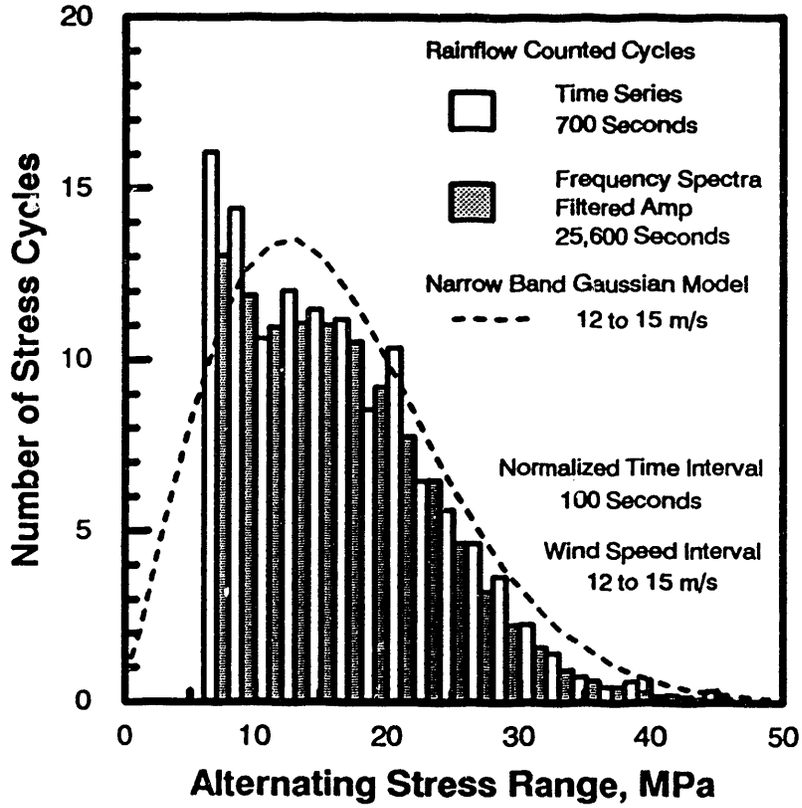

DISCLAIMER

END

DATE FILMED

12/04/91